

# Exceptionally strong double-layer barriers generated by polyampholyte salt

David Ribar,<sup>†</sup> Clifford E. Woodward,<sup>‡</sup> and Jan Forsman<sup>\*,†</sup>

<sup>†</sup>*Computational Chemistry, Lund University, P.O.Box 124, S-221 00 Lund, Sweden*

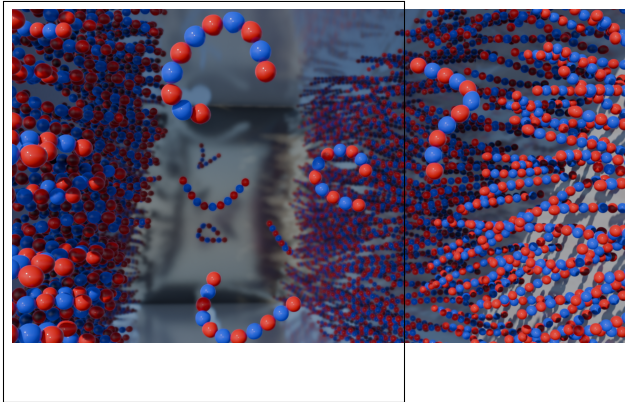
<sup>‡</sup>*School of Physical, Environmental and Mathematical Sciences University College,  
University of New South Wales, ADFA Canberra ACT 2600, Australia*

E-mail: [jan.forsman@compchem.lu.se](mailto:jan.forsman@compchem.lu.se)

## Abstract

Experiments using the Surface Force Apparatus (SFA) have found anomalously long-ranged interactions between charged surfaces in concentrated salt solutions. Ion clustering have been suggested as a possible origin of this behaviour. In this work, we demonstrate that if such stable clusters indeed form, they are able to induce remarkably strong free energy barriers, under conditions where a corresponding solution of simple salt provide negligible forces. Our cluster model is based on connected ions producing a polyampholyte salt, containing a symmetric mixture of monovalent cationic and anionic polyampholytes. Ion distributions and surface interactions are evaluated utilising statistical-mechanical (*classical*) polymer Density Functional Theory, cDFT. In the Supporting Information, we briefly investigate a range of different polymer architectures (connectivities), but in the main part of the work a polyampholyte ion is modelled as a linear chain with alternating charges, in which the ends carry an identical charge (hence, a monovalent net charge). These salts are able to generate repulsions, between similarly charged surfaces, of a remarkable strength - exceeding those from simple salts by orders of magnitude. The underlying mechanism for this is the formation of brush-like layers at the surfaces, i.e. the repulsion is strongly related to excluded volume effects, in a manner similar to the interaction between surfaces carrying grafted polymers. We believe our results are relevant not only to possible mechanisms underlying anomalously long-ranged underscreening in concentrated simple salt solutions, but also for the potential use of synthesised polyampholyte salt as extremely efficient stabilisers of colloidal dispersions.

## TOC Graphic



## Keywords

polyampholytes, electrolytes, ion clusters, simulations, anomalous screening, colloidal stability

Using simple salt to regulate the stability of colloidal dispersions that contain charged particles is a well established process, with a firm theoretical foundation.<sup>1-5</sup> Mean-field treatments of aqueous systems tends to be accurate at low and intermediate concentrations when the salts are composed of monovalent species. An important mean-field result is the so-called Debye screening length,  $\lambda_D$ , that describes the effective range of electrostatic interactions in the presence of salt. As the salt concentration increases, *ionic screening* leads to a reduced range, with  $\lambda_D \sim 1/c^{1/2}$ . However, recent experiments using the Surface Force Apparatus, SFA, indicate a peculiar non-monotonic behaviour: above a threshold concentration (usually around 1M), the range of electrostatic forces *increase* upon the addition of salt.<sup>6-9</sup> This remarkable response has some support from colloidal stability<sup>10</sup> and thin film<sup>11</sup> investigations, but there are also contradictory experiments.<sup>12</sup> Several theoretical efforts have been made to establish possible underlying molecular mechanisms<sup>13-22</sup> but there is still no broadly accepted view on the matter.

Ion pairing, or ion clusters, have been suggested to play a role for the alleged strong and long-ranged repulsion at high ionic strengths.<sup>6,20-25</sup> In this work, we investigate surface forces in the presence of aqueous solutions that contain *constructed* “ion clusters”, or at least molecular architectures that can be viewed as simple models of monovalent ion clusters. Our description is based on an implicit treatment of water, which only enters via its dielectric constant,  $\epsilon_r = 78.3$ , and ions that are connected to form “ion clusters” with a univalent net charge. This system will be treated using *classical* polymer Density Functional Theory, cDFT.

We investigate different polyampholytic architectures, but they are all composed of connected charged hard spheres with diameter,  $d$ . The bond between neighbouring charges in a cluster has a fixed length  $b$ , and allows for full rotationally flexibility. The solution is modelled using an implicit solvent, and a salt composed of an equimolar mixture of monovalent polyampholyte cations and anions. The number of charged monomers per chain is denoted

by  $r$ , with each  $r$ -mer carrying a net single elementary charge. In the main article we will consider a simple linear architecture with alternating charges along the chain. Thus, the polyampholytic cation will have positive end monomers, and a total of  $(r + 1)/2$  positive and  $(r - 1)/2$  negative charges, with the opposite true for anions. Here, we will compare surface interactions in the presence of a purely polyampholyte salt with those obtained with a simple salt.

In the Supporting Information (SI) we explore different chain architectures and charge distributions. For example, we investigate the situation where the charges are collected in blocks of monomers of the same valency. Such chains are likely adopt a folded state, unless there is additional simple salt. These architectures appear to give rise to rather dramatic effects, but we postpone their more detailed study for future work.

Non-bonded monomer-monomer interactions are denoted by  $\phi_{ij}(r)$ , where:

$$\beta\phi_{ij}(r) = \begin{cases} \infty; & r \leq d \\ l_B \frac{Z_i Z_j}{r}; & r > d \end{cases} \quad (1)$$

Here,  $\beta = (k_B T)^{-1}$  is the inverse thermal energy,  $l_B \approx 7.16 \text{\AA}$  is the Bjerrum length and  $Z_i$  and  $Z_j$  denote the valencies of interacting monomers  $i$  and  $j$  ( $|Z| = 1$  in all cases). Monomer densities are denoted  $n_+$  (cations) and  $n_-$  (anions).

We study the interactions between two flat, hard and infinitely large surfaces, carrying a surface charge density  $\sigma = -1/70 e/\text{\AA}^2$ , where  $e$  is the elementary charge. The surfaces are immersed in our model mixture and the separation  $h$  between the surfaces is varied. The system is treated using the grand canonical ensemble, i.e. the confined fluid is in chemical equilibrium with an infinite bulk. The equilibrium (minimal) free energy is obtained at each separation and the net osmotic pressure is evaluated either as a discrete free energy derivative or from the monomer contact values at the surfaces. All polymer configurations are accounted for,<sup>26</sup> subject to a Boltzmann weight, under the assumption that densities only vary in the direction transverse to the surfaces.

For a completely ideal bulk polymer solution, in which there are no particle-particle interactions or external fields, save the bond constraints, the polymer free energy,  $\mathcal{F}_p^{id}$ , for an  $r$ -mer can be *exactly* written as:

$$\beta\mathcal{F}_p^{(id)} = \int N(\mathbf{R}) (\ln[N(\mathbf{R})] - 1) d\mathbf{R} + \beta \int N(\mathbf{R}) V_b(\mathbf{R}) d\mathbf{R} \quad (2)$$

where a polymer configuration is represented by  $\mathbf{R} = (\mathbf{r}_1, \dots, \mathbf{r}_r)$ , and the density distribution  $N(\mathbf{R})$  is defined such that  $N(\mathbf{R})d\mathbf{R}$  is the number of polymer molecules having configurations between  $\mathbf{R}$  and  $\mathbf{R} + d\mathbf{R}$ .  $V_b(\mathbf{R})$  is the bond potential between connected monomers. In this work, we will only consider bonds of fixed length, i.e.  $e^{-\beta V_b(\mathbf{R})} \propto \prod \delta(|\mathbf{r}_{i+1} - \mathbf{r}_i| - b)$  where  $b$  is the bond length, and  $\delta(x)$  is the Dirac delta function.

For our model of a bulk polyampholyte salt, the Helmholtz free energy is given by:

$$\mathcal{F}(V, T, N_+, N_-) = \sum_{i=\pm} \mathcal{F}_i^{(id)} + \mathcal{F}_{HS}^{(ex)}(n_+, n_-) + \mathcal{U} \quad (3)$$

We have used the index  $i$  to indicate that there are two types of (non-ideal) chains with alternating charges, one of which (the cation) starts and ends with a positive charge. Anions will have negative ends. The *ideal* contribution to the free energy in the bulk is identical for both species, but in a heterogeneous environment they will be different. Excluded volume interactions are approximated by  $\mathcal{F}_{HS}^{(ex)}$ , and is assumed to depend only on total cationic and anionic monomer density  $n_+, n_-$ . We have used the Generalised Flory-Dimer theory to estimate this term.<sup>27,28</sup> All electrostatic interactions are collected in  $\mathcal{U}$ , and treated at the mean-field level. In our slit environment, we use the grand potential  $\Omega$ , which can be expressed using the following Legendre transformation

$$\Omega(V, T, \mu_+, \mu_-; [n_+, n_-, \sigma]) = \mathcal{F}(V, T; [n_+, n_-, \sigma, \Psi_D]) + A \sum_{i=\pm} \int (V_{ex}(z) - \mu_i) dz \quad (4)$$

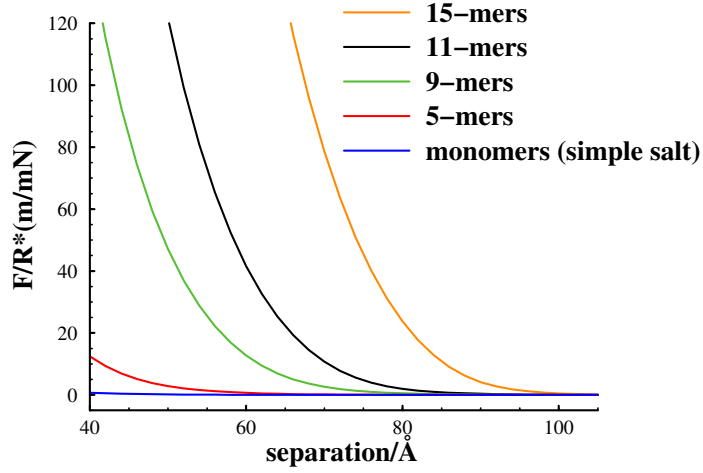
Here,  $z$  is the direction normal to the surfaces,  $A$  is the surface area, and  $\Psi_D$  is a Donnan

potential that ensures that the system is electroneutral. Polymer configurational entropy, excluded volume and electrostatic mean-field interactions (including a wall-wall repulsion) are all contained in  $\mathcal{F}$ . The cation/anion chemical potential is denoted by  $\mu_+/\mu_-$ .  $V_{ex}$  represents the non-electrostatic interaction with the confining surfaces and, as mentioned, these are purely steric in nature, so  $V_{ex}(z) = 0$  if  $d/2 < z < (h - d/2)$  and infinite elsewhere. The grand potential was minimised numerically at each separation  $h$ , to its equilibrium value,  $\Omega_{eq}(h)$ , using Picard iterations. Defining  $g_s(h) \equiv \Omega_{eq}/A - p_b h$ , where  $p_b$  is the bulk pressure, we arrive at the *net* interaction free energy as  $\Delta g_s \equiv g_s(h) - g_s(h \rightarrow \infty)$ .

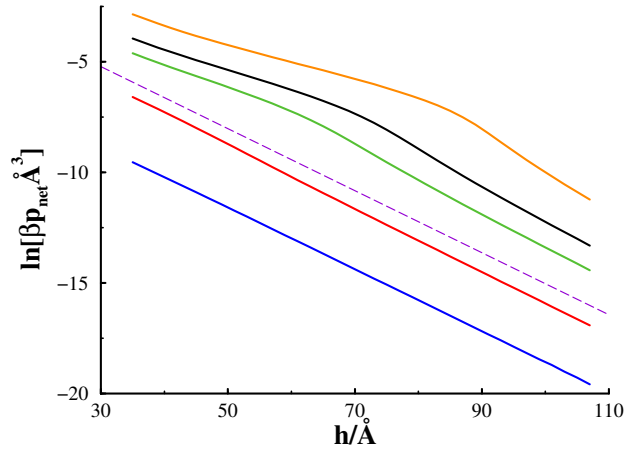
In order to compare with published SFA data, we will utilise the Derjaguin Approximation, and transform calculated net free energies per unit area to the force per radius,  $F/R$ , appropriate to the crossed cylinder setup in experiments. In that case,  $F/R = 2\pi\Delta g_s$ . The net pressure acting perpendicularly to the flat surfaces is denoted  $p_{net}$ , with  $p_{net} = -\partial\Delta g_s/\partial h$ .

In Figure 1, we compare surface interactions for simple salt, and polyampholyte salt, at a bulk salt concentration of 182mM. In the latter case, we consider monodisperse chains of increasing degree of polymerisation, while the chain concentration remains fixed at 182mM in the bulk. Such a scenario could serve as a crude approximation to a hypothetical system where ionic clusters begin to form in a simple monomeric salt (at 182mM) and any added salt only serves to increase cluster size. This type of behaviour was actually observed in recent all-atomistic MD simulations by Komori and Terao.<sup>24</sup> They found that increasing the concentration of monovalent simple salts beyond a critical value (in that case 1M) gave only an insignificant increase in the free ion concentration.

In Figure 1(a), we see a significant increase of the repulsive interaction between the charged surfaces, compared to monomeric salt, even for rather modest cluster sizes. While the polyampholyte chains are assumed to be linear, in the SI we report that quite similar results are obtained with a branched (star-like) architecture. Despite the growth in repulsion with chain length, the long-range decay of the interaction remains relatively constant. In Figure 1(b), we see that the long-ranged decay is very similar in all cases. For the case of



(a) Force per radius, between crossed cylinders.



(b) The logarithm of the net pressure.

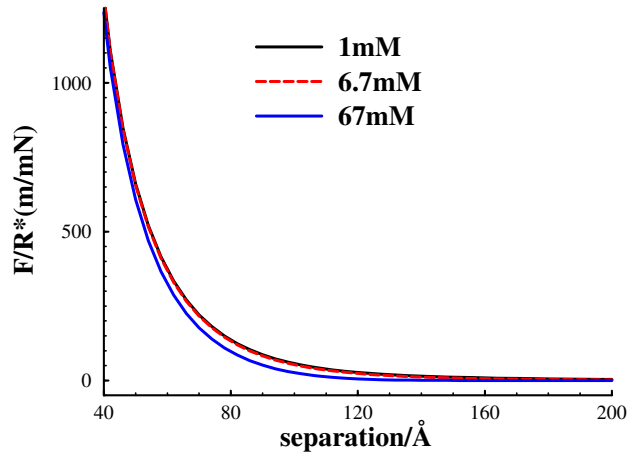
Figure 1: Surface interactions at 182mM salt concentration, for simple salts and polyampholytes of various lengths. Note that the concentration of charged monomers increase with the polymer length. For instance, with 11-mers, the bulk concentration of cationic as well as anionic monomers is 2M, but the polyampholyte *salt* concentration is still 182mM. Legend colours are the same in graph (b) as in (a). The thin dashed line in graph (b) shows a line with slope  $-1/\lambda_D(182mM)$ , where  $\lambda_D(182mM)$  is the Debye estimate of the screening length (about 7.1Å), for a 182mM aqueous solution, with a monovalent salt. The placement along the  $y$ -direction of this dashed line is arbitrarily chosen.



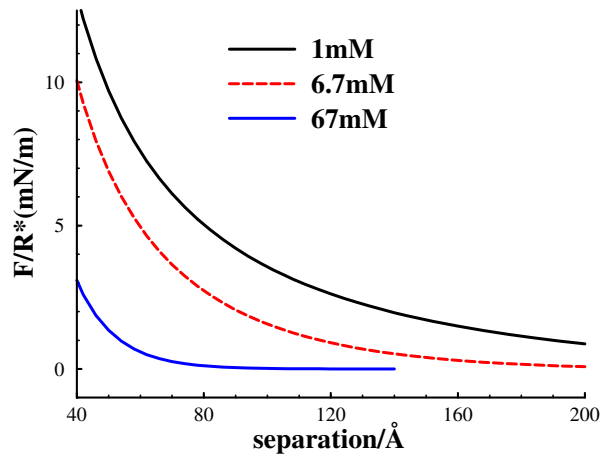
the charged monomers (simple salt), the asymptotic decay appears to be exponential, with a decay length that agrees exactly with the Debye length. This is to be expected as the *c*DFT uses mean-field electrostatics. On the other hand, there is a slight but noticeable decrease in the asymptotic decay length for the polyampholyte systems, with the decay length decreasing with cluster size. This is due to the cooperative adsorption of chains at the charged surface, which leads to more efficient screening of the surface charge compared with monomeric salt ions. We also notice that at intermediate range polyampholyte-mediated repulsion decays more slowly than with simple salt. The reason for this will be discussed below.

Another interesting property of polyampholyte salt systems is a remarkable insensitivity to changes of the concentration at short and intermediate separations. This is shown in graph Figure 2 (a), where we see how a 67-fold increase of the polyampholyte concentration leaves the surface interactions almost unchanged. This is in stark contrast to the response of simple salt solutions, illustrated in Figure 2 (b), where the same concentration increase almost eliminates the repulsion. Note the two order of magnitude difference in scale for the displayed interaction curves. This does not mean that the long-range decay length at large separations is insensitive to the concentration of polyampholyte salt though. In Figure 3 (a), we see that an increase in the polyampholyte salt concentration leads to a considerably faster decay at *large* separations. As noted above, comparisons show that the *long-ranged* decay length is very similar for polyampholyte and simple salts, Figure 3 (b).

So, where does the very strong repulsion at intermediate separations seen in the polyampholyte salts originate from? It turns out that steric interactions play a crucial role. This is exemplified in Figure 4 (a), where we note that a reduction of the monomer hard-sphere diameter leads to a dramatic drop of the surface force. This is in turn related to the monomer density distribution at the surfaces, as shown in Figure 4 (b). Only cationic monomer densities are displayed, but the overall trend is the same for anions. As the monomer radii are decreased, the chains adopt a much more compact density profile. This suggests weaker chain-chain overlap as the surfaces are brought closer together. Thus, we conclude that the



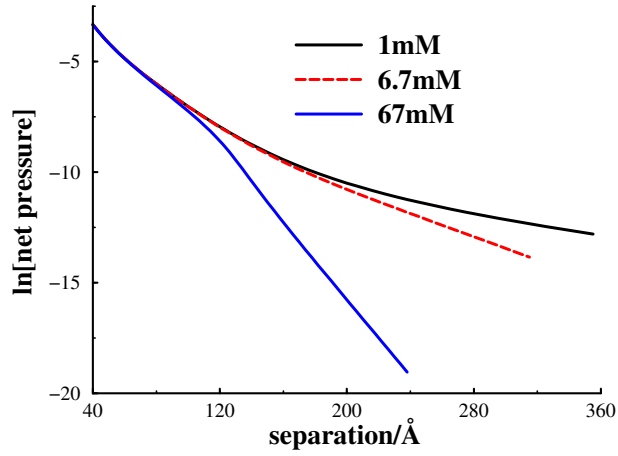
(a) 15-mer monovalent polyampholyte salt.



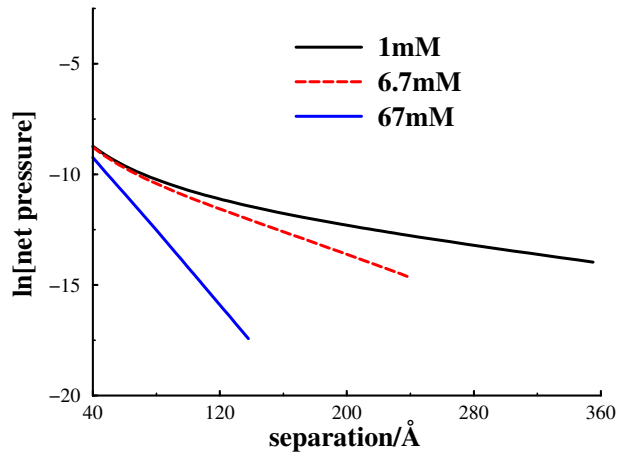
(b) Simple 1:1 salt.

Figure 2: Concentration dependence. Interaction free energies for polyampholyte (graph(a)) and simple (graph(b)) salts. Note the difference in scale between graphs (a) and (b).

strong intermediate repulsions are due to chain-chain overlaps dominated by steric interactions. In this context we note that the concentration of monomeric (simple) salt at the surfaces is generally much smaller than that of the polyampholyte monomers, leading to very weak repulsive interactions, by comparison. The apparent insensitivity of this inter-



(a) 15-mer monovalent polyampholyte salt.

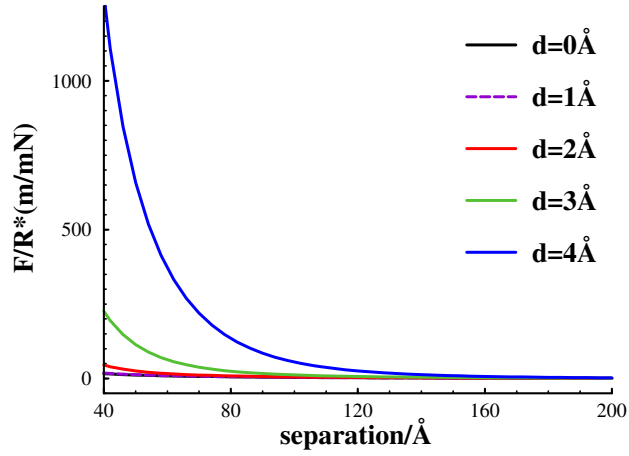


(b) Simple 1:1 salt.

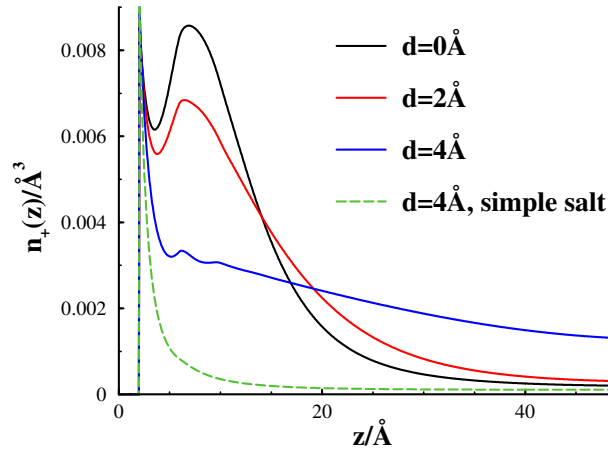
Figure 3: Concentration dependence of  $\ln[p_{net}]$ , for polyampholyte (graph(a)) and simple (graph(b)) salts.

mediate repulsion on the concentration of the polyampholyte chains means that the surface adsorption of the chains reaches saturation at fairly low concentrations.

The mechanism for this intermediate separation regime is similar to that between surfaces with adsorbed polymer layers. In that case we know that the range of the surface interactions



(a) Interaction free energies, between charged surfaces immersed in a 1mM 15-mer (monovalent) polyampholyte salt. Results are shown for polymers with monomers of sizes  $d = 0 - > 4\text{\AA}$ .



(b) Cationic monomer density profiles at one of the charged surfaces, for the same systems as in graph (a). The surface separation is  $108\text{\AA}$  in all cases.

Figure 4: Excluded volume effects, evaluated by changes to the monomer hard-sphere diameter.

is determined by the chain length. So why is this interesting? In Figure 1(b), we saw that chain-chain interactions gave rise to an intermediate decay length which was longer than the

Debye length. Though our results show that the Debye length (albeit slightly modified) was relevant at very large surface separations, our results may still have relevance to the anomalous interactions found in SFA measurements in simple concentrated salts. In this work, we have limited ourselves to chains of finite length. Thus at very large surface separations, the overlaps between finite chains are less important compared to electrostatic effects, and this is why the usual Debye-like decay of the interactions eventually prevail asymptotically. For aggregating clusters, the chain size distribution will likely have an exponential form and in this case, chain overlaps remain significant at much larger surface separations, possibly dominating the electrostatic mechanism asymptotically and giving rise to apparently anomalous long-range decays.

We envisage that our theoretical predictions are readily verifiable by surface force measurements, for instance using polypeptides that are composed of alternating amino acids of opposite charge (at some suitable pH). Upon verification, such polyampholyte salt systems could be further explored in the context of colloidal stability.

## Acknowledgement

J.F. acknowledges financial support by the Swedish Research Council, and computational resources by the Lund University computer cluster organisation, LUNARC. We also thank prof. Sture Nordholm for fruitful discussions.

## Supporting Information Available

The following files are available free of charge.

- Supporting information: Detailed simulation methods, and further analyses.
- Github repository: all codes used for simulations, along with the data generated, is freely available.

## References

- (1) Derjaguin, B. V.; Landau, L. Theory of the Stability of Strongly Charged Lyophobic Sols and of the Adhesion of Strongly Charged Particles in Solutions of Electrolytes. *Acta Phys. Chim. URSS* **1941**, *14*, 633–662.
- (2) Verwey, E. J. W.; Overbeek, J. T. G. *Theory of the Stability of Lyophobic Colloids*; Elsevier Publishing Company Inc.: Amsterdam, 1948.
- (3) Israelachvili, J. N. *Intermolecular and Surface Forces, 2nd Ed.*; Academic Press: London, 1991.
- (4) Evans, F. A.; Wennerström, H. *The colloidal domain: where Physics, Chemistry, Biology and Technology meet*; VCH Publishers: New York, 1994.
- (5) Holm, C.; Kekicheff, P.; Podgornik, R. *Electrostatic Effects in Soft Matter and Biophysics*; Kluwer Academic Publishers: Dordrecht, 2001.
- (6) Gebbie, M. A.; Valtiner, M.; Banquy, X.; Fox, E. T.; Henderson, W. A.; Israelachvili, J. N. Ionic liquids behave as dilute electrolyte solutions. *PNAS* **2013**, *110*, 9674–9679.
- (7) Gebbie, M. A.; Dobbs, H. A.; Valtiner, M.; Israelachvili, J. N. Long-range electrostatic screening in ionic liquids. *PNAS* **2015**, *112*, 7432–7437.
- (8) Smith, A. M.; Lee, A. A.; Perkin, S. The Electrostatic Screening Length in Concentrated Electrolytes Increases with Concentration. *J. Phys. Chem. Lett.* **2016**, *7*, 2157–2163.
- (9) Fung, Y. K. C.; Perkin, S. Structure and anomalous underscreening in ethylammonium nitrate solutions confined between two mica surfaces. *Faraday Discuss.* **2023**, *246*, 370–386.

- (10) Yuan, H.; Deng, W.; Zhu, X.; Liu, G.; Craig, V. S. J. Colloidal Systems in Concentrated Electrolyte Solutions Exhibit Re-entrant Long-Range Electrostatic Interactions due to Underscreening. *Langmuir* **2022**, *38*, 6164–6173.
- (11) Gaddam, P.; Ducker, W. Electrostatic Screening Length in Concentrated Salt Solutions. *Langmuir* **2019**, *35*, 5719–5727.
- (12) Kumar, S.; Cats, P.; Alotaibi, M. B.; Ayirala, S. C.; Yousef, A. A.; van Roij, R.; Siretanu, I.; Mugele, F. Absence of anomalous underscreening in highly concentrated aqueous electrolytes confined between smooth silica surfaces. *J. Colloid Interface Sci.* **2022**, *622*, 819–827.
- (13) Lee, A. A.; Perez-Martinez, C. S.; Smith, A. M.; Perkin, S. Scaling Analysis of the Screening Length in Concentrated Electrolytes. *Phys. Rev. Lett.* **2017**, *119*, 026002.
- (14) Coupette, F.; Lee, A. A.; Härtel, A. Screening Lengths in Ionic Fluids. *Phys. Rev. Lett.* **2018**, *121*, 075501.
- (15) Rotenberg, B.; Bernard, O.; Hansen, J.-P. Underscreening in ionic liquids: a first principles analysis. *J. Phys. Condens. Matter* **2018**, *30*, 054005.
- (16) Kjellander, R. A multiple decay-length extension of the Debye-Hückel theory: to achieve high accuracy also for concentrated solutions and explain under-screening in dilute symmetric electrolytes. *Phys. Chem. Chem. Phys.* **2020**, *22*, 23952–23985.
- (17) Coles, S. W.; Park, C.; Nikam, R.; Kanduc, M.; Dzubiella, J.; Rotenberg, B. Correlation Length in Concentrated Electrolytes: Insights from All-Atom Molecular Dynamics Simulations. *J. Phys. Chem. B* **2020**, *124*, 1778–1786.
- (18) Zeman, J.; Kondrat, S.; Holm, C. Bulk ionic screening lengths from extremely large-scale molecular dynamics simulations. *Chem. Commun.* **2020**, *56*, 15635–15638.

- (19) Cats, P.; Evans, R.; Härtel, A.; van Roij, R. Primitive model electrolytes in the near and far field: Decay lengths from DFT and simulations. *J. Chem. Phys.* **2021**, *154*, 124504.
- (20) Härtel, A.; Bültmann, M.; Coupette, F. Anomalous Underscreening in the Restricted Primitive Model. *Phys. Rev. Lett.* **2023**, *130*, 108202.
- (21) Elliott, G. R.; Gregory, K. P.; Robertson, H.; Craig, V. S.; Webber, G. B.; Wanless, E. J.; Page, A. J. The known-unknowns of anomalous underscreening in concentrated electrolytes. *Chemical Physics Letters* **2024**, *843*, 141190.
- (22) Ribar, D.; Woodward, C. E.; Forsman, J. Long-ranged double-layer forces at high ionic strengths, with a modified Restricted Primitive Model. *submitted to Phys. Rev. Res.*
- (23) Ma, K.; Forsman, J.; Woodward, C. E. Influence of ion pairing in ionic liquids on electrical double layer structures and surface force using classical density functional approach. *The Journal of Chemical Physics* **2015**, *142*, 174704.
- (24) Komori, K.; Terao, T. Cluster-size distribution of ions in concentrated aqueous NaCl solutions: Molecular dynamics simulations. *Chemical Physics Letters* **2023**, *825*, 140627.
- (25) Ribar, D.; Woodward, C. E.; Nordholm, S.; Forsman, J. Cluster Formation Induced by Local Dielectric Saturation in Restricted Primitive Model Electrolytes. *J. Phys. Chem. Lett.* **2024**, *15*, 8326–8333.
- (26) Woodward, C. E. Density functional theory for inhomogeneous polymer solutions. *J. Chem. Phys.* **1991**, *94*, 3183.
- (27) Wichert, J. M.; Gulati, H. S.; Hall, C. K. Binary hard chain mixtures I. Generalized Flory equations of state. *J. Chem. Phys.* **1996**, *105*, 7669.
- (28) Forsman, J.; Woodward, C. E. Evaluating the accuracy of a density functional theory



of polymer density functional theory of polymer solutions with additive hard sphere diameters. *J. Chem. Phys.* **2004**, *120*, 506.

# SUPPORTING INFORMATION FOR:

## Exceptionally strong double-layer barriers generated by polyampholyte salt

David Ribar<sup>a</sup> , Clifford E. Woodward<sup>b</sup> , Jan Forsman<sup>a,\*</sup> 

<sup>a</sup> *Computational Chemistry, Lund University, P.O.Box 124, S-221 00 Lund, Sweden*

<sup>b</sup> *School of Physical, Environmental and Mathematical Sciences University College, University of New South Wales, ADFA Canberra ACT 2600, Australia*

\*Corresponding author: [jan.forsman@compchem.lu.se](mailto:jan.forsman@compchem.lu.se)

(Dated: 2024-12-04)

### S1 Model illustration

We have constructed a cartoon illustration of our polyampholyte salt model. It is shown, for 5-mer

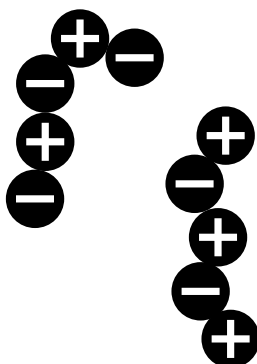


Figure 1: A graphical illustration of a cation and an anion, in a 5-mer polyampholyte salt.

polyampholytes, in Figure 1. This is for a case where the hard-sphere diameter  $d$  equals the bond length  $b$ , i.e.  $d = b = 4\text{\AA}$ . In the main paper, we also considered cases with smaller monomers.

### S2 Other polymer architectures

Here we will briefly consider other modelling options for the polyampholytes, which we recall also might serve as a crude description of ion clusters. One might anticipate a rather compact arrangement of an ion cluster, and a step in that direction would be to allow the polymers to become star-like, with several branches connecting to a common central monomer. However, we see in Figure 2 that the resulting interaction free energies are quite similar for branched and linear polymer architectures. Moreover, distributing the single net charge per chain uniformly among the monomers leads to quite similar results as for monovalent polyampholytes in which the monomers have alternating charge. On the other hand, if the charges are collected into two separate blocks with opposing valency (one block containing one more monomer than the other), then the repulsive force become much stronger. One should then keep in mind that the construction of such polymers in a “real” solution might lead to folded structures, at least for

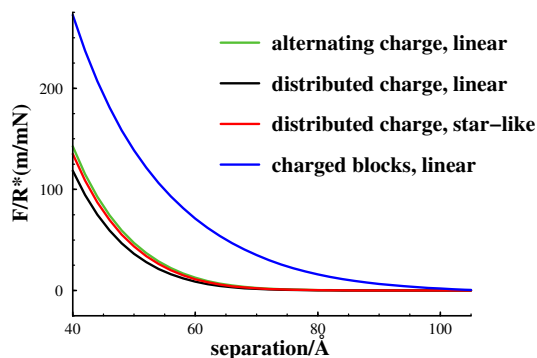


Figure 2: Interactions between charged surfaces, immersed in a solution containing 182mM 9-mer polyampholyte salts. The green curve are results using our reference model (main paper), i.e. composed of monomers with alternating charge. We also display (black) results using linearly connected chains with a single charge that is equally distributed between the monomers ( $\pm e/9$  charge per monomer, resulting in monovalent chains). In the latter case, we furthermore show (red) corresponding interactions when the polymers have a 4-armed star structure, i.e. 4 branches connecting to a common central monomer. Finally, the blue curve shows interactions in the presence of polymers with a linear block charge structure (+ + + + - - - - and + + + + - - - -).

large degrees of polymerisation. The tendency to fold can be counteracted by the addition of simple salt, and interactions in the presence of such salt mixtures will be the focus of a future work.

Let us finally illustrate the relevance of excluded volume interactions, also when the monovalent charge is evenly distributed among the monomers, and when the polymers have a star-like structure. This is

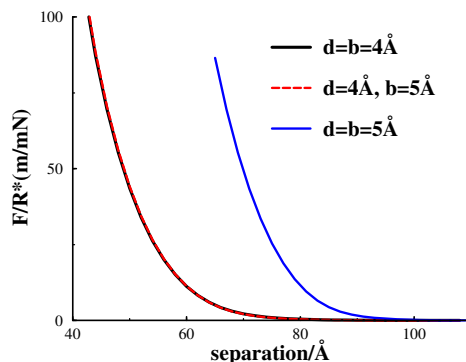


Figure 3: Interactions between charged surfaces, immersed in a solution containing 182mM 9-mer polyampholyte salts. Here, we consider chains with a 4-armed star structure, and various choices for the bond length ( $b$ ) and monomer hard-sphere diameter ( $d$ ).

illustrated in Figure 3, under conditions similar to those in Figure 2, i.e. 182mM monovalent 9-mer salt. We note that for a given monomer diameter, the bond length has a weak influence. On the other hand, increasing the hard-sphere monomer diameter generates a dramatically stronger repulsion.